Excitation Dynamics of Two Spectral Forms of the Core Complexes from Photosynthetic Bacterium *Thermochromatium tepidum*

Fei Ma,*† Yukihiro Kimura,‡ Xiao-Hui Zhao,*† Yi-Shi Wu,*† Peng Wang,† Li-Min Fu,† Zheng-Yu Wang,‡ and Jian-Ping Zhang*†

*Beijing National Laboratory for Molecular Science, State Key Laboratory for Structural Chemistry of Unstable and Stable Species, Institute of Chemistry, Chinese Academy of Sciences, Beijing, China; †Department of Chemistry, Renmin University of China, Beijing, China; and ‡Faculty of Science, Ibaraki University, Mito, Japan

ABSTRACT The intact core antenna-reaction center (LH1-RC) core complex of thermophilic photosynthetic bacterium *Thermochromatium* (*Tch.*) *tepidum* is peculiar in its long-wavelength LH1-Q_y absorption (915 nm). We have attempted comparative studies on the excitation dynamics of bacteriochlorophyll (BChl) and carotenoid (Car) between the intact core complex and the EDTA-treated one with the Q_y absorption at 889 nm. For both spectral forms, the overall Car-to-BChl excitation energy transfer efficiency is determined to be ~20%, which is considerably lower than the reported values, e.g., ~35%, for other photosynthetic purple bacteria containing the same kind of Car (spirilloxanthin). The RC trapping time constants are found to be 50~60 ps (170~200 ps) for RC in open (closed) state irrespective to the spectral forms and the wavelengths of Q_y excitation. Despite the low-energy LH1-Q_y absorption, the RC trapping time are comparable to those reported for other photosynthetic bacteria with normal LH1-Q_y absorption at 880 nm. Selective excitation to Car results in distinct differences in the Q_y-bleaching dynamics between the two different spectral forms. This, together with the Car band-shift signals in response to Q_y excitation, reveals the presence of two major groups of BChls in the LH1 of *Tch. tepidum* with a spectral heterogeneity of ~240 cm^{-1}, as well as an alteration in BChl-Car geometry in the 889-nm preparation with respect to the native one.

INTRODUCTION

The photosynthetic unit of purple photosynthetic bacteria consists of a reaction center (RC) enclosed by a core antenna (LH1) referred to as the LH1-RC core complex, and a variable number of peripheral antenna complexes (LH2). Light absorbed by the antenna complexes is followed by the LH2 → LH1 → RC migration of electronic excitation, which is eventually trapped by the RC and is utilized to drive the primary charge separation (1–4). The recent crystallographic structures of RC and LH2 complexes have revealed the detailed molecular basis of a model photosynthetic unit: the structures of RCs from *Blastochloris* (*Bl.*) *viridis* (5), *Rhodobacter* (*Rb.*) *sphaeroides* (6), and *Thermochromatium* (*Tch.*) *tepidum* (7) with spatial resolutions of ~2 Å, those of LH2 from *Rhodopseudomonas* (*Rps.*) *acidophila* 10050 (8,9), and *Rhodospirillum* (*Rs.*) *molischianum* (10) with 2.0~2.5 Å, as well as the structure of LH1-RC from *Rps. palustris* with a moderate resolution of 4.8 Å (11).

The Q_y absorption maxima of bacteriochlorophyll-*a* (BChl) in different antenna complexes, LH1 and LH2~4, may locate at 800, 820, 850, or 880 nm, depending on the strain to BChl molecule exerted by proteic binding via axial-ligation and/or hydrogen-bond interactions, on the strength of excitonic coupling among BChls, as well as on the electrostatic interactions with surroundings (12–14). A striking feature of the Q_y absorption is the considerably large bathochromic shift with reference to BChl free in organic solvent (e.g., ~780 nm in acetone). The characters of the electronic excitation residing on the BChl aggregates in the LH1 or LH2 antenna, e.g., the excitonic interactions, the length of excitation delocalization, and the inter- or intraband excitation dynamics, etc., have been subjected to extensive experimental and theoretical studies (for recent reviews, see (14,15)). It is interesting to see that, for a few purple photosynthetic bacteria such as *Tch. tepidum* ATCC 43061^T (16), *Rss. parvum* DSMZ 12498^T (17), and the strain 970 (18), respectively, the LH1-Q_y absorption maxima even exceed 900 nm, i.e., ~915, ~909, and ~963 nm. Despite the unusual long-wavelength BChl absorption, the LH1-to-RC excitation energy transfer (EET) or RC trapping timescales are similar to those of *Rs. rubrum* or *Rb. sphaeroides* with the normal LH1-Q_y absorption at ~880 nm. E.g., the RC trapping time are 55 ± 5 ps and 65 ± 5 ps for the chromatophores of *Rss. parvum* (4) and strain 970 (18), respectively. Here, the independence of the RC trapping time on the Q_y-state energy of BChls in LH1 remains to be fully understood.

Tch. tepidum grows in a temperature range of 48~50°C (19). Its LH1-RC complex exhibits notably higher thermal stability than the mesophilic counterparts such as *Allochromatium* (*Ach.*) *vinosum*, *Rb. sphaeroides*, and *Bl. viridis* growing under ~30°C (20). In addition, the Q_y absorption of the intact LH1-RC complex from *Tch. tepidum* shifts from ~915 nm to ~885 nm when the complex elutes in the presence of NaCl, KCl, KBr, NaCl, or $MgCl_2$ (150 mM) and, interestingly, the 885-nm spectral form can be fully converted back to the 915-nm one by adding $CaCl_2$ (16,21).

Submitted March 19, 2008, and accepted for publication May 7, 2008.

Address reprint requests to Jian-Ping Zhang, Tel.: 86-10-62-51-66-04; E-mail: jpzhang@chem.ruc.edu.cn.

Editor: Brian R. Dyer.

0006-3495/08/10/3349/09 $2.00

doi: 10.1529/biophysj.108.133835

Recently, the polypeptides of LH1 complex have been purified and the amino-acid sequences determined (22). In addition, the dimeric feature of BChls, the highly symmetric LH1-ring assembly as well as the BChl-carotenoid (Car) interaction, have been confirmed (23). Furthermore, it has been shown that spirilloxanthin is the major Car composition (92.3%), and that the pigment-protein assembly of the 889-nm preparation is thermally less stable than that of the native one (21,23).

The fully reversible 915-nm and 889-nm spectral forms of LH1-RC complex from *Tch. tepidum* provide an opportunity to investigate the structure-function relationship. This work is attempted to compare the dynamics and efficiency of RC trapping and Car-to-BChl EET processes between the different LH1-RC preparations. It is found that the RC trapping efficiency is ~94% for either of the two preparations, and is independent on the excitation photon energy. In addition, the Car-to-BChl overall EET efficiency is ~20%, which is considerably lower than those reported for other bacterial species. Although no obvious difference in RC trapping and in Car-to-BChl EET efficiency are found between the 915-nm and the 889-nm preparations, distinct difference are observed in the LH1-Q_y bleaching dynamics upon Car excitation as well as in the Car band-shift signals upon Q_y excitation. These are discussed in terms of the spectral heterogeneity among BChls and the variation in BChl-to-Car relative orientation in the two LH1-RC spectral forms.

MATERIALS AND METHODS

Preparation of LH1-RC complexes

Chromatophore was isolated by sonication of the whole cell of *Tch. tepidum* suspended in 20 mM Tris-HCl buffer (pH = 8.5) followed by differential centrifugation. The chromatophore was extracted with 0.35% (w/v) LDAO at 25°C for 60 min, followed by centrifugation for 90 min at 4°C (150,000 × *g*). The LH1-RC complex from *Tch. tepidum* with the LH1-Q_y absorption maximum at 915 nm was prepared following previously reported procedures (22). This preparation is considered to be intact since the chromatophore originally exhibits the LH1-Q_y absorption maximum at ~915 nm (Fig. 1 *a*). The 889-nm preparation, i.e., the LH1-RC complex with the LH1-Q_y absorption maximum at ~889 nm (Fig. 1 *b*), was prepared by adding 200 mM EDTA into the intact 915-nm preparation. For spectroscopic measurements, the LH1-RC preparations or the chromatophore were suspended in buffer (pH = 7.5) containing 20 mM Tris-HCl and 0.8% (w/v) β-OG. For time-resolved spectroscopic experiments, the optical densities of the LH1-RC preparations or chromatophore suspension were adjusted to ~0.45 mm^{-1} at selected pumping wavelengths. Open-state condition of RC was achieved by adding 20 mM ascorbate together with 2 μM phenazine methosulfate (3).

Spectroscopic measurements

The ultraviolet (UV)-visible absorption and the fluorescence excitation spectra, respectively, were recorded on spectrophotometers U3310 and F4500 (Hitachi, Pleasanton, CA), for which the protein or chromatophore samples were diluted to 2 μM in buffer.

The femtosecond time-resolved absorption spectrometer had been described elsewhere (24). Briefly, an optical parametric amplifier (OPA-800 CF, Spectra-Physics Lasers, Mountain View, CA) pumped by a regenerative amplifier (Spitfire, Spectra-Physics Lasers) provided the actinic laser pulses (~120 fs, full width at half-maximum), and the pulse energy was 100 nj/pulse corresponding to a photon density of 10^{14} photons/pulse × cm^2 in the sample cell (optical path length, 1 mm). White light continuum generated from a 3-mm thick sapphire plate was used as the probe, which was detected by a liquid-nitrogen cooled charge-coupled device detector (Spectrum-1, Jy Inc., SPEX Forensics, Edison, NJ) attached to an imaging spectrometer (270 M, SPEX Forensics). For the pump-probe measurements, the magic-angle scheme was adopted, and the temporal resolution was ~150 fs. Time-resolved spectra were corrected against group velocity dispersion. To ensure that each laser-shot excited a fresh sample, the laser system was run at a repetition rate of 5 Hz, and the sample cell was kept shifting across the actinic beams. All of the measurements were carried out at room temperature.

RESULTS AND DISCUSSION

Steady-state spectroscopy

Fig. 1 shows the UV-visible absorption spectra of the LH1-RC complexes. The bands of Car (0−0 vibronic transition at

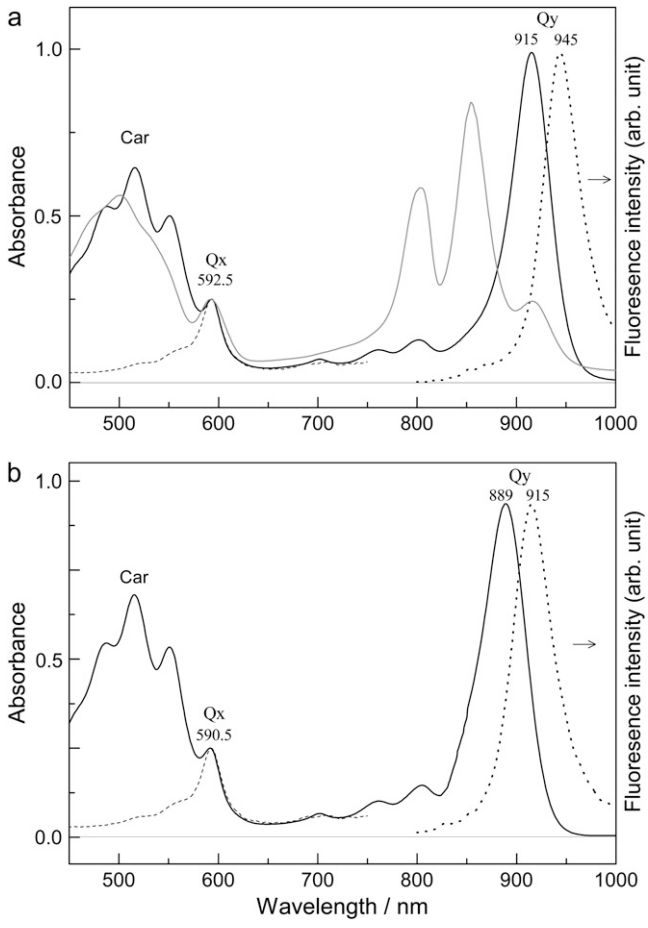

FIGURE 1 Room temperature UV-visible (*solid*), fluorescence (*dotted*) and fluorescence excitation (*dashed*) spectra of (*a*) the 915-nm and (*b*) the 889-nm LH1-RC preparations from *Tch. tepidum*. Observing wavelengths for fluorescence excitation spectra were 945 nm in panel *a* and 915 nm in panel *b*. Absorption and fluorescence excitation spectra are normalized at the Q_x absorption maxima. UV-visible spectrum of the chromatophore (*shaded*) is shown in panel *a* for comparison.

550 nm) and those of accessory BChl (~800 nm) or bacteriopheophytin (~760 nm) in RC exhibit no distinct difference between the 915-nm and the 889-nm preparations, indicating that either the Car in LH1 or the pigment cofactors in RC have little structural and environmental variation. However, compared to the intact LH1-RC, the Q_x and Q_y absorption of the 889-nm preparation shift to the blue for 2 nm (14 cm^{-1}) and 26 nm (320 cm^{-1}), respectively, and the Q_y bandwidth increases slightly (46 nm vs. 52 nm, or 560 cm^{-1} vs. 690 cm^{-1}). These spectral differences reflect significant changes in the BChl microenvironment in the two different preparations.

For either 915-nm or 889-nm preparations, the overall efficiency of Car-to-BChl singlet EET is ~20% as determined at 550 nm from the steady-state fluorescence excitation and electronic absorption spectra (Fig. 1). This value is considerable lower than those reported for the chromatophore of *Tch. tepidum* (~30%) (25), for the native LH1-RC from *Rs. rubrum* (28~35%) (26–28), as well as for the LH1 from *Rs. rubrum* G9 reconstituted with spirilloxanthin (36~40%) (28,29). The divergence in the Car-to-BChl EET efficiency is likely due to the variation in sample preparations; e.g., the LH1-RC complexes from *Tch. tepidum* in this work are highly purified ones (that is, have no complication from peripheral antenna complexes, as in the case of chromatophore).

For the two LH1-RC preparations from *Tch. tepidum*, the similarity in Car-to-BChl overall EET efficiency can be explained below. The Car(S_1)-to-BChl(Q_y) EET path is essentially inactive (see below) and, therefore, a significant change in the energy of the acceptor Q_y-state would not affect the overall EET efficiency appreciably. As for the predominant EET path of Car(S_2 or S*)-to-BChl(Q_x), a 2-nm shift of the Q_x absorption would not result in any significant change in the spectral overlap between the donor emission and the acceptor absorption; this, together with the presumably unchanged Car-BChl coupling, leads to a similar overall efficiency.

BChl excited-state dynamics and RC trapping dynamics upon Q_y excitation

Fig. 2, panels *a* and *b*, respectively, depicts the representative transient spectra of the 915-nm and the 889-nm preparations with RC in open state. Both cases show the excited-state absorption (ESA) peaked at ~885:865 nm, the bleaching of ground state absorption (BLC) at ~915:890 nm, as well as the stimulated emission (SE) at ~940:920 nm. Though the key spectral features of the two sets of transients are similar, distinct differences can be recognized:

1. An isosbestic wavelength of ~897 nm appears at 100 fs for the 915-nm preparation (Fig. 2 *a*), whereas that of ~878 nm is reached at 200 fs for the 889-nm one (Fig. 2 *b*). The delay in spectral equilibrium may reflect slower relaxation of higher-lying excitonic states of BChls in the 889-nm preparation.
2. Comparing the 400-fs transients, the relative SE intensity at ~920 nm in Fig. 2 *b* is higher than that at ~940 nm in Fig. 2 *a*. Here, it is worth noting that, for either of the two preparations, the relative SE intensities were higher in the cases with closed RC (data not shown), which is understandable in view of the decrease in the amount of quench centers (active RCs).

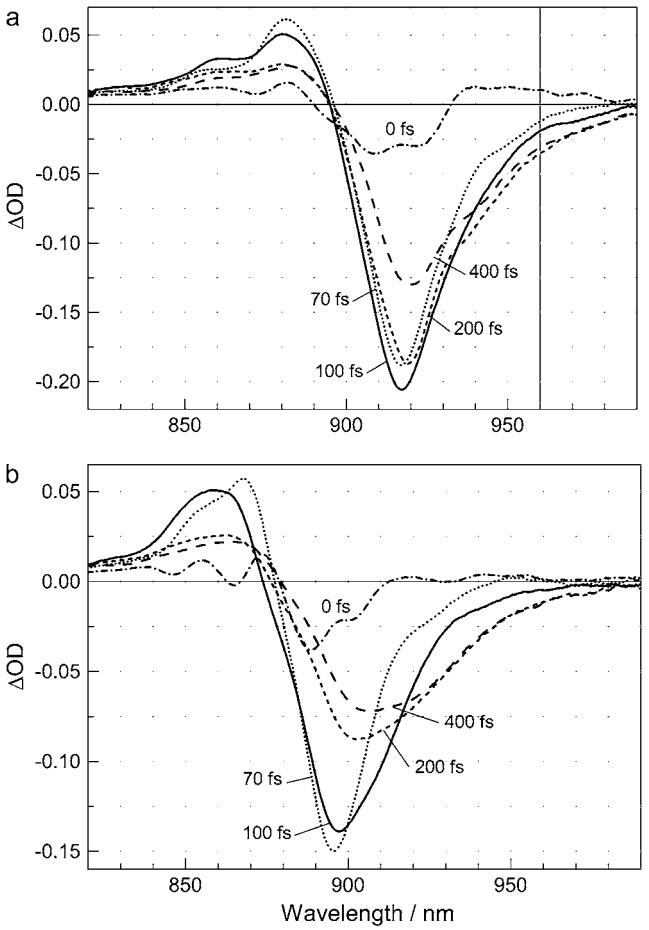

FIGURE 2 Difference absorption spectra at indicated delay times for (*a*) the 915-nm and (*b*) the 889-nm LH1-RC preparations from *Tch. tepidum* with RC in open state. Excitation wavelength was 915 nm in panel *a* and 895 nm in panel *b*.

Fig. 3 shows the kinetics of excited-state BChls at indicated probing wavelengths along with the fitting curves derived from a bi-exponential model function. For both preparations, the shorter- and the longer-wavelength kinetics probe the ESA and the BLC of BChls, respectively. To examine the effect of excitation photon energy on the rate of RC trapping reactions, three excitation wavelengths at 895, 915, and 930 nm were used. Table 1 lists the time constants obtained under various combinations of probe and excitation wavelengths.

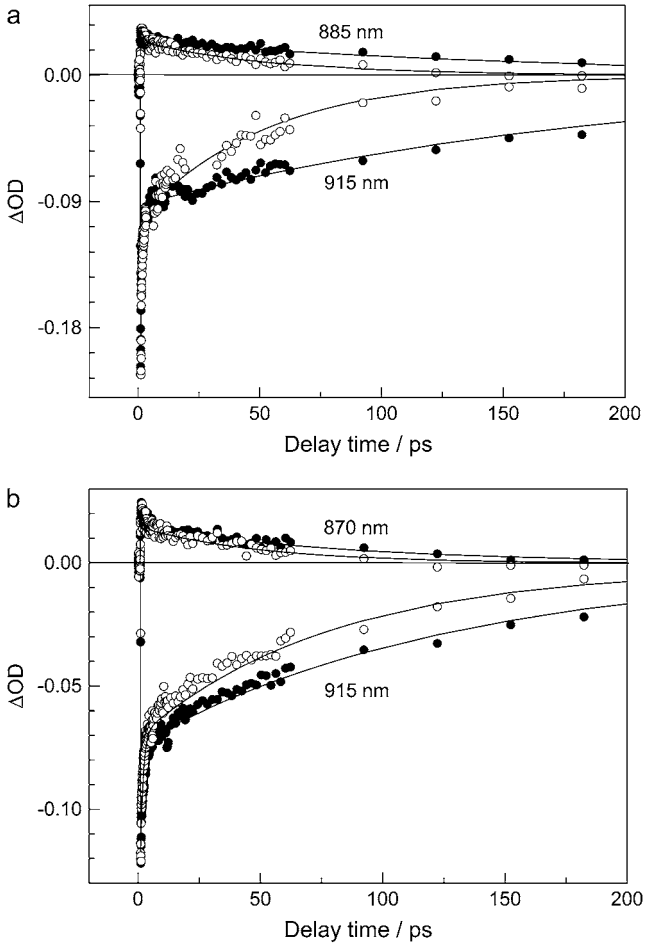

FIGURE 3 Kinetics traces at the indicated probing wavelengths for (*a*) the 915-nm and (*b*) the 889-nm preparations of LH1-RC complexes from *Tch. tepidum* in open (*open circle*) and closed (*solid circle*) states. Solid lines are fitting curves. Excitation wavelength was 915 nm in panel *a* and 895 nm in panel *b*.

It is seen from Table 1 that τ_1 is, on average, <2.5 ps for both preparations with RC, either in open or closed states. This fast decay component, also clearly seen from the kinetics in Fig. 3, may originate from the following processes:

1. Depopulation owing to excitation annihilation that is plausible in view of this regime of excitation photon density (10^{14} photons/pulse $\times$ cm^2);
2. Spectral equilibration owing to the relaxation of higher-lying excitonic states, the dynamic Stokes shift of SE process and the intraband EET process among BChls (see below).

These processes are also responsible for the aforementioned sub-picosecond spectral equilibration in Fig. 2. The slower decay component, τ_2, which is distinctly different for RC in open and closed states (Table 1, Fig. 3), is the result of RC trapping (time constants, τ_{tr}) competing with the $S_1(Q_y)$-to-S_0 internal conversion (IC) of BChls in LH1 (time constants, τ_0).

As determined by means of time-resolved fluorescence spectroscopy, τ_0 for LH1 is typically ~1 ns (30). This work has derived τ_2 from the kinetics curve fittings, thus τ_{tr} can be obtained according to the relation $\tau_2^{-1} = \tau_{tr}^{-1} + \tau_0^{-1}$, and the results are summarized in Table 1. It is seen that the trapping time of open-state RC (~60 ps) is approximately one-third of that of closed-state RC (~180 ps), in agreement with literature values of other purple bacteria such as *Rs. rubrum* and *Rb. sphaeroides* (3). For both preparations with open RC, the trapping efficiencies of 94% is obtained by using the relation $\eta = \tau_{tr}^{-1}/\tau_2^{-1}$.

The RC trapping timescales determined in this work differ from those reported for the chromatophore of *Tch. tepidum*, i.e., 140 ps and 310 ps for open and closed RCs, respectively (31). We also measured the chromatophore with an excitation of 590 nm as used in Kennis et al. (31), and τ_{tr} was found to be 55.4 ps for open RC. The apparent discrepancy may originate from the difference in other experimental conditions, e.g., in Kennis et al. (31) the time resolution was 15~25 ps and no detergent was used for the chromatophore suspension. Nevertheless, the RC trapping time of ~60 ps for either 915-nm or 889-nm preparations from *Tch. tepidum* is similar to those found for other purple bacteria bearing long-wavelength LH1-Q_y absorption, e.g., ~55 ps for *Rss. parvum* absorbing at 909 nm, and 65 ps for strain 970 absorbing at 963 nm (4,18). It is intriguing that the RC trapping time for purple bacteria is rather uniform irrespective to the energetic locations of the LH1-Q_y absorption.

For the 915-nm (889-nm) preparation of LH1-RC complex from *Tch. tepidum*, the LH1-Q_y absorption is ~630 cm^{-1} (~310 cm^{-1}) lower in energy with respect to the special pair in RC with maximal absorption at ~865 nm, and the optical excitation at 930 nm corresponds to an even larger energy difference of ~ 800 cm^{-1}. Furthermore, varying the LH1-Q_y excitation from 895 nm to 930 nm also did not alter the RC trapping time (Table 1). As the energy differences, 300~800 cm^{-1}, are significantly larger than the kT energy, ~220 cm^{-1} at 25°C, the unchanged rate of LH1-to-RC uphill EET is rather puzzling.

The uphill excitation energy trapping for purple photosynthetic bacteria has been well known (32–35). The temperature dependence of the trapping rate have been examined (32,36), and the rate at room temperature is found to be rather uniform over a wide range of uphill energy gaps (4,18,32,33, 35). Recent theoretical studies (34,35) have revealed a thermally activated sequential mechanism of RC trapping for *Rb. sphaeroides* having smaller energy gap (~200 cm^{-1}), i.e., EET from LH1 to special pair followed by the primary charge separation, as well as a superexchange mechanism at low temperature for *Rhodopseudomonas* (*Rps.*) *viridis* having a larger energy gap (350~400 cm^{-1}), i.e., the special pair serves as a virtual mediator in an one-step trapping process directly leading to the initial charge separation. Despite the extensive experimental and theoretical studies, the uniformity in the trapping rate against energy gap remains to be fully understood.

TABLE 1 Decay time constants (τ_1, τ_2) obtained by exponential curve fitting to the kinetics traces (see Fig. 3) at different probing/excitation wavelengths (λ_{pr} and λ_{ex}) for the 915-nm and the 889-nm preparations of LH1-RC from *Tch. tepidum*; the RC trapping time constant is τ_{tr} (see text for details)

			Open			Closed		
LH1-RC preparation	λ_{ex} (nm)	λ_{pr} (nm)	τ_1 (ps)	τ_2 (ps)	τ_{tr} (ps)	τ_1 (ps)	τ_2 (ps)	τ_{tr} (ps)
915-nm form	895	885	1.2 ± 0.6	58.3 ± 5.6	61.9	1.9 ± 0.4	149.0 ± 8.6	175.1
	915		1.4 ± 0.2	54.9 ± 2.1	58.1	1.7 ± 0.2	166.0 ± 6.7	199.0
	930		1.4 ± 0.3	48.1 ± 5.2	50.5	1.6 ± 0.1	158.0 ± 3.1	187.6
	895	915	0.6 ± 0.0	59.4 ± 1.8	63.2	0.8 ± 0.0	160.3 ± 4.6	190.9
	915		0.5 ± 0.0	51.3 ± 1.7	54.1	0.7 ± 0.0	164.2 ± 7.0	196.5
	930		0.1 ± 0.0	54.2 ± 2.9	57.3	1.0 ± 0.1	153.3 ± 7.4	181.1
889-nm form	895	870	2.1 ± 0.2	48.3 ± 3.6	50.8	2.3 ± 0.2	143.0 ± 5.5	166.9
	915		1.3 ± 0.1	50.8 ± 2.8	53.5	2.3 ± 0.2	150.0 ± 3.6	176.5
	930		2.4 ± 0.9	53.5 ± 6.1	56.5	1.6 ± 0.3	143.0 ± 7.8	166.9
	895	915	1.1 ± 0.0	55.4 ± 1.9	58.6	1.2 ± 0.0	160.2 ± 2.7	190.8
	915		1.0 ± 0.1	57.4 ± 8.2	60.9	1.1 ± 0.1	161.1 ± 13.6	192.0
	930		0.2 ± 0.0	59.4 ± 5.0	63.2	0.4 ± 0.01	144.5 ± 2.7	169.0

BChl and Car excited-state dynamics upon Car excitation

Fig. 4 shows the near-infrared (NIR), time-resolved difference absorption spectra recorded after Car excitation at 550 nm. Compared to Fig. 2, a striking feature in spectral dynamics is that no isosbestic wavelengths and, therefore, no spectral equilibration are reached in the delay-time range up to 4 ps, which may be due to the involvement of an intermediate Car(S*), living for a few picoseconds, in the Car-to-BChl EET process (see below). Thus the excited-state dynamics of BChl in response to Car excitation is more complicated than the case of Q_y excitation, which is not surprising, upon considering the involvement of both the Car-to-BChl EET and the Car ESA processes.

The spectral dynamics in Fig. 4, *a* and *b*, are further compared and discussed below. For both preparations, broad Car($S_n \leftarrow S_2$) ESA extending over 960 nm (37) appears and starts to decay after the Car excitation. Simultaneously, broad ESA (820~900 nm in Fig. 4 *a* and 820~875 nm in Fig. 4 *b*) and BLC (900~970 nm in Fig. 4 *a* and 875~970 nm in Fig. 4 *b*) of BChls emerge and begin to rise. The decay-to-rise correlation reflects the process of EET from the higher-lying excited states of Car(S_2 and/or S*) to the Q_x state of BChl.

For the 915-nm preparation (Fig. 4 *a*), the transient spectra earlier than 100 fs exhibit dual BLC bands peaked at ~900 nm and ~920 nm with a energy separation of ~240 cm^{-1}, which develop into a single band at ~920 nm at the delay time of ~100 fs. From 100 fs to 4.0 ps, the BLC signal further shifts to red for ~5 nm. Compared to the 915-nm preparation, the 889-nm one also shows dual BLC bands at ~890 nm and ~910 nm; however, distinct differences can be recognized:

1. The dual-band structure is more prominent, and the red-edge SE signal in the 4.0-ps transient is relatively stronger.
2. Decay of the higher energy band in Fig. 4 *b* (~400 fs) is much slower than that in Fig. 4 *a* (~100 fs).
3. Importantly, the decay of the higher energy band (~890 nm) shows an apparent correlation to the rise of the lower energy band (~910 nm), as further proven by the kinetics in Fig. 5 obtained by decomposing the transient spectra in Fig. 4 *b* into two Gaussian components.

Structured BLC dynamics had been observed under cryogenic temperature and Q_y excitation for the LHCII complex from higher plant (38), reflecting the EET between energetically different Chl molecules in various microenvironments. In addition, spectral heterogeneity but not distinct BLC bands had also been found at 77 K and Q_y excitation for the core complex from *Rps. viridis* (39). Therefore, this observation of distinct BLC band structure on Car excitation and at room temperature is new and rather interesting. The ~240 cm^{-1} spectral heterogeneity may originate from the BChls bound to the α- and β-polypeptides. As supporting evidence, subtle difference in BChl molecular structure such as macrocycle planarity has been shown by the x-ray crystallographic data for the LH2 or the LH-RC complexes (8,9,11). The spectral heterogeneity is not visible in the steady-state absorption spectra owing to the broad bandwidths of BChl absorption in the LH complexes (500~600 cm^{-1}) that are larger than the spectral heterogeneity observed in this work (~240 cm^{-1}). Furthermore, the absence of distinct dual-band structure upon Q_y excitation (compare to Fig. 2) can be ascribed to the nonselective excitation of BChls with the optical pulses having a bandwidth as large as ~10 nm (full width at half-maximum).

The dual band structures observed on Car excitation, but not LH1-Q_y excitation, are apparently induced by the Car-to-BChl EET. With this in mind, the spectral dynamics in Fig. 4 and the kinetics in Fig. 5 are interpreted below. Either the intact or the 889-nm preparations contain two groups of BChls with a spectral heterogeneity of ~240 cm^{-1}. The faster decaying higher energy bands may be attributed to the

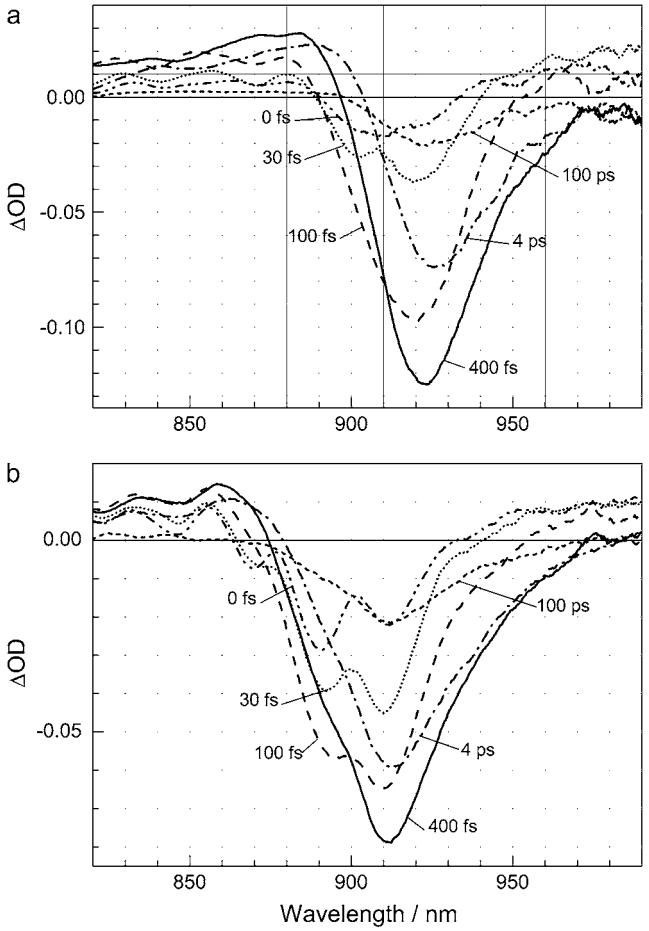

FIGURE 4 Difference absorption spectra at indicated delay times for (*a*) the 915-nm and (*b*) the 889-nm preparations of open-state LH1-RC complexes from *Tch. tepidum*. Excitation wavelength was 550 nm for both cases.

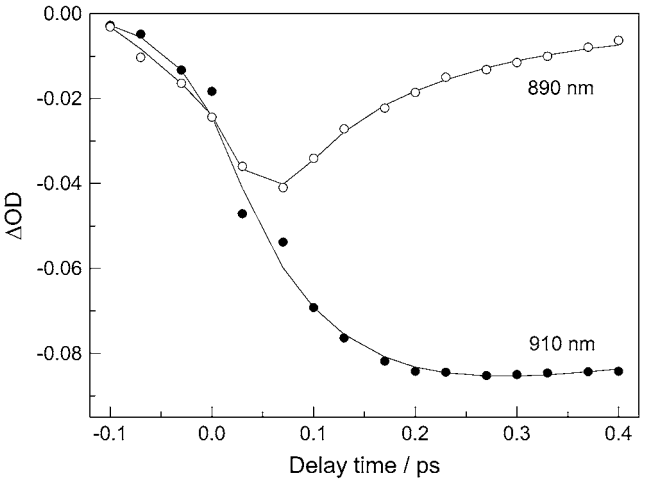

FIGURE 5 Kinetics traces for the LH1-Q_y bleaching bands at 890 nm and 910 nm (see Fig. 4 *b*). They were obtained by decomposition of the BLC spectra assuming two spectral components with Gaussian line shape. The solid curves are to guide the eye. Excitation wavelength was 550 nm.

intraband EET between the two groups of BChls; however, the decay-to-rise kinetics correlation (Fig. 5) does not necessarily reflect the direct intraband EET process, since Car-to-BChl EET also contributes to the rise of the 910-nm kinetics. On the other hand, the recovery of the 890-nm kinetics must be merely induced by the intraband EET among BChls, whose timescale is estimated to be ~100 fs.

Regarding the Car-to-BChl EET for spirilloxanthin in the LH1 antenna, recent studies had revealed a number of new findings, e.g., the formation of ^{3}Car* on a subpicosecond timescale via the singlet fission reaction from the literature (27,29,40–42), and the involvement of an intermediate Car(S*) in the EET process (41,42). Based on these advances and the kinetics data presented in Fig. 6, we would like to briefly comment on the issue of Car-to-BChl EET. The kinetics traces at 616 nm in Fig. 6 *a* probe the Car(S_1) state, which can be well described by a bi-exponential model function. A rising component with $\tau_1 \approx 230$ fs is ascribed to the S_2-to-S_1 IC process, while the other component decaying with $\tau_2 \approx 1.5$ ps is assigned to the S_1-state lifetime (27). Because the Car(S_1) lifetime of spirilloxanthin is not shortened in LH1 with respect to that of free spirilloxanthin, we conclude that the Car(S_1)-to-BChl(Q_y) EET path is inactive, which may be explained in terms of the rather weak Car(S_1)-BChl(Q_y) coupling owing to the vanishingly small oscillator strength of the donor state and/or the unfavorable Car-BChl molecular geometry. However, since the Car(S_1) energy of spirilloxanthin in LHs is ~11,500 cm^{-1} (43), which is ~570 cm^{-1} (~250 cm^{-1}) higher than the BChl(Q_y) energy in the 915-nm (889-nm) preparation, the Car(S_1)-to-BChl(Q_y) EET seems energetically feasible.

The kinetics at 575 nm in Fig. 6 *a* probing Car(S*) (27) can be well accounted for by a three-exponential model function with a rise phase of $\tau_1 \approx 350$ fs and two decay ones of $\tau_2 \approx 4.7$ ps and $\tau_3 \sim 1$ ns. The rise time (350 fs) of Car(S*) is distinctly different from that of IC to Car(S_1) (230 fs) as clearly seen from Fig. 6 *a*, a fact suggesting that the S* and the S_1 states are not parallel-populated from the S_2 state. The time constant $\tau_2 \approx 4.7$ ps is attributed to the Car(S*) lifetime since it agrees with the reported value for spirilloxanthin in LH1 (27,40), whereas the time constant $\tau_3 \sim 1$ ns may be ascribed to the long-lived excited state BChl and/or Car species (27).

In Fig. 6 *b*, the kinetics at 960-nm probing Car(S_2) and those at 865- or 885-nm probing BChl(Q_y) show apparent decay-to-rise correlations. However, simply based on the pairs of kinetics curves, we cannot derive any definitive Car-to-BChl EET rates or efficiency, because the Car(S_2) and the Car(S*) dynamics as well as the intraband BChl dynamics all contribute to these particular kinetics. Although the detailed Car-to-BChl EET scheme awaits further investigation, the following can be concluded. The Car-to-BChl EET schemes are similar between the 915-nm and the 889-nm preparations, because their kinetics behaviors resemble each other closely, as seen in Fig. 6 *a*. In addition, the timescale of Car-to-BChl

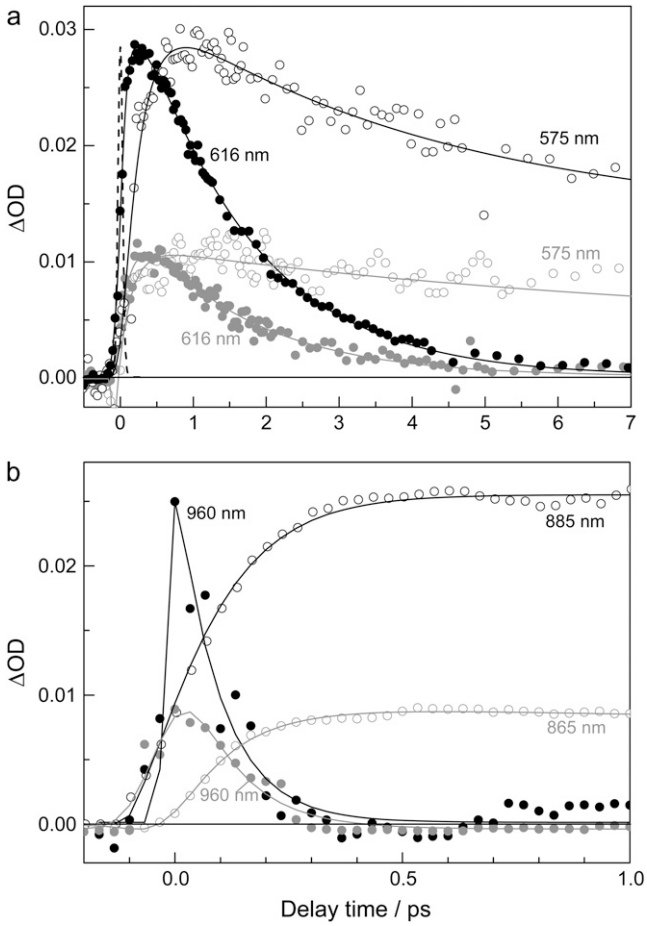

FIGURE 6 Kinetics traces followed the pulsed excitation at 550 nm. (*a*) Kinetics traces at visible probing wavelengths. The dashed line shows a Gaussian-type instrumental response function, and solid lines are fitting curves. (*b*) Kinetics traces at NIR probing wavelengths. Solid lines are to guide the eye. In both cases, the kinetics data for the 915-nm and the 889-nm preparations are shown in solid and in shaded representation, respectively. Both preparations of the LH1-RC complexes were in open state.

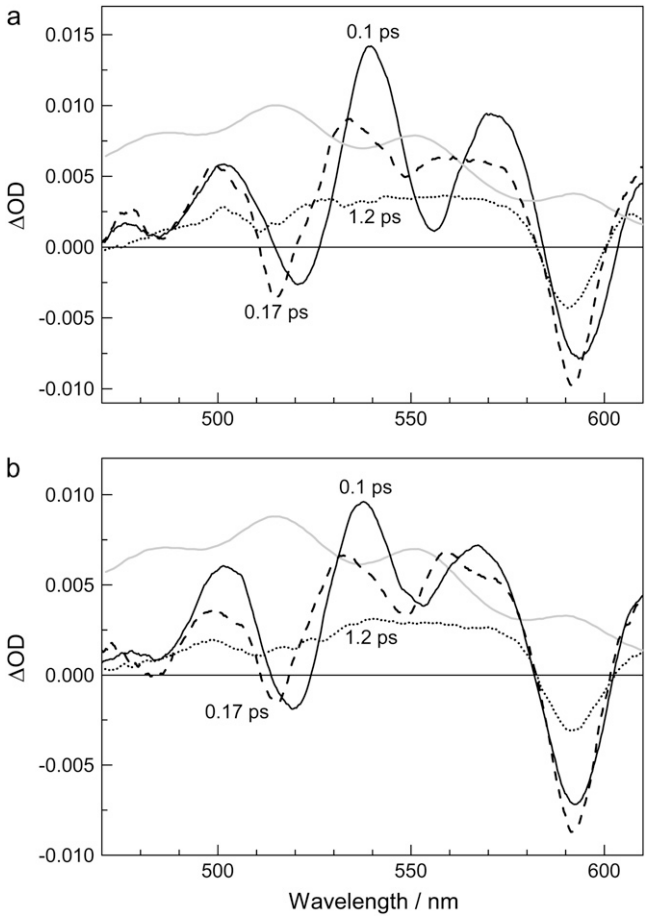

FIGURE 7 Transient spectra in visible spectral region at indicated delay times for (*a*) the 915-nm and (*b*) the 889-nm preparations of the LH1-RC complexes from *Tch. tepidum* in open state. Excitation wavelength was 915 nm. The UV-visible absorption spectra are shown in shaded curves for reference.

EET must be in the subpicosecond regime, judging from the rise phase of the ESAs in Fig. 6 *b*.

Car band shift in response to Q_y excitation

In response to the excited-state dynamics of BChls, Car neurosporene in the LH2 from *Rb. sphaeroides* was found to change in its $S_2 \leftarrow S_0$ transition energy, appearing as a dynamic band shift signal, which can be a sensitive probe for the local environment changes (44–46). Similar phenomena were observed in this work for both LH1-RC preparations from *Tch. tepidum* (Fig. 7): Upon LH1-Q_y excitation at 915 nm, transient signals of Car appear in the wavelength range at $<$590 nm. For both preparations, the Car signals reach maximal amplitude at 0.1 ps, and shift systematically to the blue at 0.17 ps. These signals decay-out at 1.2 ps, leaving the featureless ESA signals of BChls. Compared to the 889-nm preparation, the 915-nm one shows a more prominent structure of the Car signal, with slightly narrower bandwidth and larger blue-shift.

It had been reported that the response of Car to the BChl excitations is considerably weaker in the LH2 from *Rs. molischianum* than in that from *Rps. acidophila*, and that the Car-BChl distance is one of the determinants to the amplitude and pattern of the Car band-shift signal (45). Compared to the 915-nm preparation, the aforementioned differences in the Car band-shift signals imply weaker Car-BChl* interaction in the 889-nm one, which further means that the Car-BChl distances and/or the relative orientation can be slightly different between the two spectral forms of LH1-RC complexes.

In bacterial antenna, the optical absorption of Car is known to be sensitive to the nonspecific and specific interactions with the environments, e.g., electrostatic attraction, π-π stacking with the aromatic amino-acid residues, hydrophobic and hydrogen-bond interactions (47). The UV-visible Car absorption spectra are nearly identical for both LH1-RC preparations (compare to Fig. 1). In addition, the circular dichroism spectra of Car also show no difference between the

two preparations (21). Therefore, the protein environment of Car are unchanged from 915-nm to 889-nm preparations. Thus the difference in the Car band-sift signals for the two LH1-RC preparations observed in this work may reflect the subtle alteration in the BChl geometrical orientations.

CONCLUSIONS

We have studied the excited-state dynamics of BChls in the structurally correlated intact and EDTA-treated LH1-RC complexes from *Tch. tepidum* with LH-Q_y absorption maxima at 915 nm and 889 nm, respectively. The RC trapping process and the excited-state dynamics of BChl are compared by examining the NIR spectral dynamics upon optical excitation with different photon energies. In addition, the Car band-shift signals in response to the LH1-Q_y excitation is used to probe the information on BChl-Car geometry. Despite the difference in the LH1-Q_y energy, the two spectral forms of LH1-RC complexes exhibit similar efficiency of RC trapping or Car-to-BChl EET, and the rate of RC trapping is similar to that of photosynthetic purple bacteria having normal LH1-Q_y absorption. These results may imply that the pigment-protein assembly of LH1- RC complex has considerable allowance of structural variation to carry out its physiological functions.

This work has been supported by the Natural Science Foundation of China (grants No. 20703067 and No. 20673144) and by the Natural Science Foundation of China-Japan Society for the Promotion of Science joint project (grant No. 20711140133).

REFERENCES

1. Cogdell, R. J., A. T. Gardiner, A. W. Roszak, C. J. Law, J. Southall, and N. W. Isaacs. 2004. Rings, ellipses and horseshoes: how purple bacteria harvest solar energy. *Photosynth. Res.* 81:207–214.
2. Damjanović, A., T. Ritz, and K. Schulten. 1999. Energy transfer between carotenoids and bacteriochlorophylls in light-harvesting complex II of purple bacteria. *Phys. Rev. E Stat. Phys. Plasmas Fluids Relat. Interdiscip. Topics.* 59:3293–3311.
3. Trissl, H. W., C. J. Law, and R. J. Cogdell. 1999. Uphill energy transfer in LH2-containing purple bacteria at room temperature. *Biochim. Biophys. Acta.* 1412:149–172.
4. Permentier, H. P., S. Neerken, K. A. Schmidt, J. Overmann, and J. Amesz. 2000. Energy transfer and charge separation in the purple nonsulfur bacterium *Roseospirillum parvum*. *Biochim. Biophys. Acta.* 1460:338–345.
5. Deisenhofer, J., O. Epp, I. Sinning, and H. Michel. 1995. Crystallographic refinement at 2.3 Å resolution and refined model of the photosynthetic reaction center from *Rhodopseudomonas viridis*. *J. Mol. Biol.* 246:429–457.
6. Ermler, U., G. Fritzsch, S. K. Buchanan, and H. Michel. 1994. Structure of the photosynthetic reaction center from *Rhodobacter sphaeroides* at 2.65 Å resolution: cofactors and protein-cofactor interactions. *Structure.* 2:925–936.
7. Nogi, T., I. Fathir, M. Kobayashi, T. Nozawa, and K. Miki. 2000. Crystal structures of photosynthetic reaction center and high-potential iron-sulfur protein from *Thermochromatium tepidum*: thermostability and electron transfer. *Proc. Natl. Acad. Sci. USA.* 97:13561–13566.
8. McDermott, G., S. M. Prince, A. A. Freer, A. M. Hawthornthwaite-Lawless, M. Z. Papiz, R. J. Cogdell, and N. W. Isaacs. 1995. Crystal structure of an integral membrane light-harvesting complex from photosynthetic bacteria. *Nature.* 374:517–521.
9. Papiz, M. Z., S. M. Prince, T. Howard, R. J. Cogdell, and N. W. Isaacs. 2003. The structure and thermal motion of the B800–850 LH2 complex from *Rps. acidophila* at 2.0 Å resolution and 100 K: new structural features and functionally relevant motions. *J. Mol. Biol.* 326:1523–1538.
10. Koepke, J., X. C. Hu, C. Muenke, K. Schulten, and H. Michel. 1996. The crystal structure of the light-harvesting complex II (B800–850) from *Rhodospirillum molischianum*. *Structure.* 4:581–597.
11. Roszak, A. W., T. D. Howard, J. Southall, A. T. Gardiner, C. J. Law, N. W. Isaacs, and R. J. Cogdell. 2003. Crystal structure of the RC-LH1 core complex from *Rhodopseudomonas palustris*. *Science.* 302:1969–1972.
12. Olsen, J. D., J. N. Sturgis, W. H. J. Westerhuis, G. J. S. Fowler, C. N. Hunter, and B. Robert. 1997. Site-directed modification of the ligands to the bacteriochlorophylls of the light-harvesting LH1 and LH2 complexes of *Rhodobacter sphaeroides*. *Biochemistry.* 36:12625–12632.
13. Cogdell, R. J., T. D. Howard, N. W. Isaacs, K. McLuskey, and A. T. Gardiner. 2002. Structural factors which control the position of the Q_y absorption band of bacteriochlorophyll *a* in purple bacterial antenna complexes. *Photosynth. Res.* 74:135–141.
14. Sundström, V., T. Pullerits, and R. van Grondelle. 1999. Photosynthetic light-harvesting: reconciling dynamics and structure of purple bacterial LH2 reveals function of photosynthetic unit. *J. Phys. Chem. B.* 103:2327–2346.
15. van Grondelle, R., and V. I. Novoderezhkin. 2006. Energy transfer in photosynthesis: experimental insights and quantitative models. *Phys. Chem. Chem. Phys.* 8:793–807.
16. Fathir, I., M. Ashikaga, K. Tanaka, T. Katano, T. Nirasawa, M. Kobayashi, Z. Y. Wang, and T. Nozawa. 1998. Biochemical and spectral characterization of the core light harvesting complex 1 (LH1) from the thermophilic purple sulfur bacterium *Chromatium tepidum*. *Photosynth. Res.* 58:193–202.
17. Tuschak, C., J. T. Beatty, and J. Overmann. 2004. Photosynthesis genes and LH1 proteins of *Roseospirillum parvum* 930I, a purple nonsulfur bacterium with unusual spectral properties. *Photosynth. Res.* 81:181–199.
18. Permentier, H. P., S. Neerken, J. Overmann, and J. Amesz. 2001. A bacteriochlorophyll *a* antenna complex from purple bacteria absorbing at 963 nm. *Biochemistry.* 40:5573–5578.
19. Madigan, M. T. 1984. A novel photosynthetic purple bacterium isolated from a Yellowstone Hot Spring. *Science.* 225:313–315.
20. Watson, A. J., A. V. Hughes, P. K. Fyfe, M. C. Wakeham, K. Holden-Dye, P. Heathcote, and M. R. Jones. 2005. On the role of basic residues in adapting the reaction center-LH1 complex for growth at elevated temperatures in purple bacteria. *Photosynth. Res.* 86:81–100.
21. Kimura, Y., Y. Hirano, L. J. Yu, H. Suzuki, M. Kobayashi, and Z. Y. Wang. 2008. Calcium ions are involved in the unusual red-shift of LH1 Q_y transition of the core complex from Thermophilic purple sulfur bacterium *Thermochromatium tepidum*. *J. Biol. Chem.* 283:13867–13873.
22. Wang, Z. Y., M. Shimonaga, H. Suzuki, M. Kobayashi, and T. Nozawa. 2003. Purification and characterization of the polypeptides of core light-harvesting complexes from purple sulfur bacteria. *Photosynth. Res.* 78:133–141.
23. Suzuki, H., Y. Hirano, Y. Kimura, S. Takaichi, M. Kobayashi, K. Miki, and Z. Y. Wang. 2007. Purification, characterization and crystallization of the core complex from thermophilic purple sulfur bacterium *Thermochromatium tepidum*. *Biochim. Biophys. Acta.* 1767:1057–1063.
24. Han, R. M., Y. S. Wu, J. Feng, X. C. Ai, J. P. Zhang, and L. H. Skibsted. 2004. Radical cation generation from singlet and triplet excited states of all-*trans*-lycopene in chloroform. *Photochem. Photobiol.* 80:326–333.

25. Kramer, H., and J. Amesz. 1996. Antenna organization in the purple sulfur bacteria *Chromatium tepidum* and *Chromatium vinosum*. *Photosynth. Res.* 49:237–244.

26. Davis, C. M., P. L. Bustamante, and P. A. Loach. 1995. Reconstitution of the bacterial core light-harvesting complexes of *Rhodobacter sphaeroides* and *Rhodospirillum rubrum* with isolated α- and β-polypeptides, bacteriochlorophyll *a*, and carotenoid. *J. Biol. Chem.* 270:5793–5804.

27. Gradinaru, C. C., J. T. M. Kennis, E. Papagiannakis, I. H. M. van Stokkum, R. J. Cogdell, G. R. Fleming, R. A. Niederman, and R. van Grondelle. 2001. An unusual pathway of excitation energy deactivation in carotenoids: singlet-to-triplet conversion on an ultrafast timescale in a photosynthetic antenna. *Proc. Natl. Acad. Sci. USA.* 98:2364–2369.

28. Nakagawa, K., S. Suzuki, R. Fujii, A. T. Gardiner, R. J. Cogdell, M. Nango, and H. Hashimoto. 2008. Probing binding site of bacteriochlorophyll *a* and carotenoid in the reconstituted LH1 complex from *Rhodospirillum rubrum* S1 by Stark spectroscopy. *Photosynth. Res.* 95:339–344.

29. Akahane, J., F. S. Rondonuwu, L. Fiedor, Y. Watanabe, and Y. Koyama. 2004. Dependence of singlet-energy transfer on the conjugation length of carotenoids reconstituted into the LH1 complex from *Rhodospirillum rubrum* G9. *Chem. Phys. Lett.* 393:184–191.

30. Campillo, A. J., R. C. Hyer, T. G. Monger, W. W. Parson, and S. L. Shapiro. 1977. Light collection and harvesting processes in bacterial photosynthesis investigated on a picosecond time scale. *Proc. Natl. Acad. Sci. USA.* 74:1997–2001.

31. Kennis, J. T. M., T. J. Aartsma, and J. Amesz. 1994. Energy trapping in the purple sulfur bacteria *Chromatium vinosum* and *Chromatium tepidum*. *Biochim. Biophys. Acta.* 1188:278–286.

32. Kleinherenbrink, F. A. M., G. Deinum, S. C. M. Otte, A. J. Hoff, and J. Amesz. 1992. Energy transfer from long-wavelength absorbing antenna bacteriochlorophylls to the reaction center. *Biochim. Biophys. Acta.* 1099:175–181.

33. Trissl, H. W. 1993. Long-wavelength absorbing antenna pigments and heterogeneous absorption bands concentrate excitons and increase absorption cross section. *Photosynth. Res.* 35:247–263.

34. Sumi, H. 2002. Uphill energy trapping by reaction center in bacterial photosynthesis: charge separation unistep from antenna excitation, virtually mediated by special-pair excitation. *J. Phys. Chem. B.* 106: 13370–13383.

35. Sumi, H. 2004. Uphill energy trapping by reaction center in bacterial photosynthesis. 2. Unistep charge separation, virtually mediated by special pair, by photoexcitation in place of excitation transfer from the antenna system. *J. Phys. Chem. B.* 108:11792–11801.

36. Visscher, K. J., H. Bergström, V. Sundström, C. N. Hunter, and R. van Grondelle. 1989. Temperature dependence of energy transfer from the long wavelength antenna BChl-896 to the reaction center in *Rhodospirillum rubrum*, *Rhodobacter sphaeroides* (w.t. and M21 mutant) from 77 to 177K, studied by picosecond absorption spectroscopy. *Photosynth. Res.* 22:211–217.

37. Zhang, J. P., L. H. Skibsted, R. Fujii, and Y. Koyama. 2001. Transient absorption from the $1B_u^+$ state of all-trans-β-carotene newly identified in the near-infrared region. *Photochem. Photobiol.* 73:219–222.

38. Novoderezhkin, V. I., M. A. Palacios, H. van Amerongen, and R. van Grondelle. 2005. Excitation dynamics in the LHCII complex of higher plants: modeling based on the 2.72 Å crystal structure. *J. Phys. Chem. B.* 109:10493–10504.

39. Monshouwer, R., A. Baltuška, F. van Mourik, and R. van Grondelle. 1998. Time-resolved absorption difference spectroscopy of the LH-1 antenna of *Rhodopseudomonas viridis*. *J. Phys. Chem. A.* 102:4360–4371.

40. Papagiannakis, E., J. T. M. Kennis, I. H. M. van Stokkum, R. J. Cogdell, and R. van Grondelle. 2002. An alternative carotenoid-to-bacteriochlorophyll energy transfer pathway in photosynthetic light harvesting. *Proc. Natl. Acad. Sci. USA.* 99:6017–6022.

41. Wohlleben, W., T. Buckup, J. L. Herek, R. J. Cogdell, and M. Motzkus. 2003. Multichannel carotenoid deactivation in photosynthetic light harvesting as identified by an evolutionary target analysis. *Biophys. J.* 85:442–450.

42. Papagiannakis, E., I. H. M. van Stokkum, M. Vengris, R. J. Cogdell, R. van Grondelle, and D. S. Larsen. 2006. Excited-state dynamics of carotenoids in light-harvesting complexes. 1. Exploring the relationship between the S_1 and S* state. *J. Phys. Chem. B.* 110:5727–5736.

43. Papagiannakis, E., I. H. M. van Stokkum, R. van Grondelle, R. A. Niederman, D. Zigmantas, V. Sundström, and T. Polívka. 2003. A near-infrared transient absorption study of the excited-state dynamics of the carotenoid spirilloxanthin in solution and in the LH1 complex of *Rhodospirillum rubrum*. *J. Phys. Chem. B.* 107:11216–11223.

44. Herek, J. L., T. Polívka, T. Pullerits, G. J. S. Fowler, C. N. Hunter, and V. Sundström. 1998. Ultrafast carotenoid band shifts probe structure and dynamics in photosynthetic antenna complexes. *Biochemistry.* 37:7057–7061.

45. Herek, J. L., M. Wendling, Z. He, T. Polívka, G. Garcia-Asua, R. J. Cogdell, C. N. Hunter, R. van Grondelle, V. Sundström, and T. Pullerits. 2004. Ultrafast carotenoid band shifts: experiment and theory. *J. Phys. Chem. B.* 108:10398–10403.

46. Zhang, J. P., H. Nagae, P. Qian, L. Limantara, R. Fujii, Y. Watanabe, and Y. Koyama. 2001. Localized excitations on the B850a and B850b bacteriochlorophylls in the LH2 antenna complex from *Rhodospirillum molischianum* as probed by the shifts of the carotenoid absorption. *J. Phys. Chem. B.* 105:7312–7322.

47. Wang, Y. L., and X. C. Hu. 2002. A quantum chemistry study of binding carotenoids in the bacterial light-harvesting complexes. *J. Am. Chem. Soc.* 124:8445–8451.